Scale of Mixing in a Stirred Vessel

A. W. RICE, H. L. TOOR, and F. S. MANNING

Carnegie Institute of Technology, Pittsburgh, Pennsylvania

Although stirred vessels are widely used in chemical technology, they have been characterized almost exclusively by empirical methods, for example power absorption per unit volume (*11*) or mixing time for tracers (*5, 13*). Recently several theoretical approaches have used turbulence theory, for example Corrsin (*4*) on an idealized turbulent mixer; Batchelor (*1*), Batchelor, Howells, and Townsend (*2*) and Beek and Miller (*3*) on the spectral decay of scalar property fluctuations; and Manning and Wilhelm (*7, 8*) on concentration fluctuations.

The present work investigates simultaneous mixing and reaction of a basic tracer stream with a surrounding acid medium. A steady state condition is achieved by continuously introducing a tracer sodium hydroxide solution into an acid stream which flows slowly upward through the stirred vessel. Both base and acid streams contain phenolphthalein indicator; hence the distance from the impeller required for complete reaction of tracer solution is visually measurable. Any realistic and detailed description of this exceedingly complex shearing and interlarding of the reacting streams by the impeller blades would be prohibitively complicated even if the additional effects of molecular diffusion and reaction are not considered. A first-order and necessarily very crude solution is now obtained with an extremely idealized model which may even be accused of being too much of a simplification. The model assumes:

1. The impeller action reduces the entering tracer stream to very thin packets. Simultaneously the shearing or other action of the blades interlards the tracer packets with the bulk circulating stream.
2. The above shearing and interlarding processes occurs very quickly, that is before the fluid is ejected from the impeller.
3. After the impeller is left, no further shearing occurs, and the acid base reaction is now controlled by molecular diffusion as outlined by Toor (*12*).

Within the impeller, effects such as flow patterns, jet mixing of the entering streams, effective eddy diffusivities, etc. are not considered separately. Their combined action is expressed in terms of packet size and subsequent reaction time. In the effluent stream only mixing on the molecular level is considered to enhance chemical reaction; larger scale eddies have little effect. If eddies in stirred vessels are similar to those in pipes, their dimensions are quite large, of the order of vessel diameter, impeller diameter, blade size, etc. Reaction of the basic tracer streaks in the effluent stream is now considered quantitatively.

THEORY

The flat-bladed turbine impeller produces a horizontal fluid sheet that maintains its radial direction until it reaches the vessel wall. At the wall the flow divides into doughnut-shaped circulation patterns above and below the impeller. There are two mixing processes in the vessel, the basic tracer with the acid recirculation stream at the impeller and the recirculating stream with the fresh entering acid at the bottom of the vessel.

Within the confines of the impeller the tracer solution is pictured as being sheared into very thin elements (slabs, cylinders, or spheres) which are then surrounded by the recirculating stream. Reaction between these interlarded layers of acid and base then occurs when the mixture leaves the impeller and becomes part of the horizontal fluid sheet. This acid-base reaction is immeasurably fast; hence the reaction rate is controlled by mass transfer considerations, that is by the diffusion of bulk acid into the basic tracer elements and vice versa. The times required for complete reaction of slabs, cylinders, or spheres with an infinite stagnant medium have been calculated by Toor (*12*) who assumed equal diffusivities. Solutions are presented as a graph relating a reduced time of reaction dimensionless group $Z_f = \dfrac{4\,Dt}{h^2}$ with a concentration ratio group C_A/C_B (Figure 6).

If the flow pattern in the horizontal sheet is assumed to be strictly two dimensional, the continuity equation for incompressible fluids requires

$$q(r) = K/r \tag{1}$$

The constant K is evaluated by assuming that at the impeller blade tip the radial fluid velocity equals the tangential velocity of the impeller blade tips. Thus

$$q(r = r_o) = 2\pi r_o N_r/60 = K/r_o \tag{2}$$

Substituting the result in Equation (1) one obtains

$$q = 2\pi r_o^2 N_r/60\, r \tag{3}$$

A. W. Rice is at Princeton University, Princeton, New Jersey.

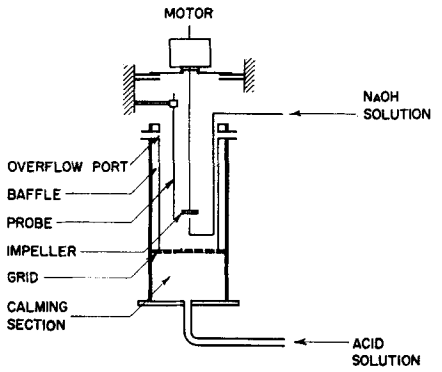

Fig. 1. Mixing vessel.

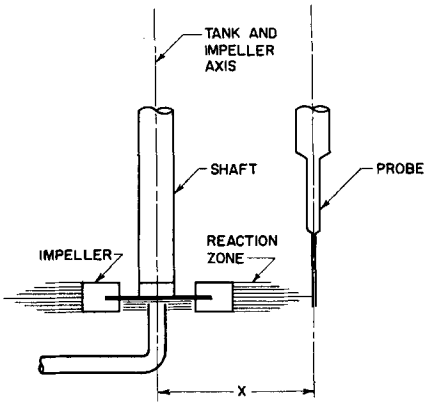

Fig. 2. Impeller and reaction zone.

In spite of the many assumptions involved this velocity profile may be verified at least in the horizontal plane passing through the center of the impeller blades for distances up to half way between the blade tip and the vessel wall. The data of Nagata (9) and Manning and Wilhelm (7) have been used to compute ($60\,q_r\,r/2\,\pi\,r_o^2\,N_r$). Results are shown in Table 1, where the model is seen to hold approximately (that is $60\,q_r\,r/2\,\pi\,r_o^2\,N_r = 1$). Hence radial distances from the impeller were converted to times of reaction by the use of Equation (3).

EXPERIMENTAL

Description of equipment, experimental procedure, and reduction of data are now presented. Greater detail is available elsewhere (*10*).

The mixing vessel is shown in Figure 1. A dilute acid (nitric acid or sulfuric acid) solution is pumped through a rotameter into a calming section, through the cylindrical primary mixing column which is 10 in. I.D. by 15 in. long, and finally through the overflow ports. This mixing section is separated from the calming section by a grid containing many closely-spaced holes. A sodium hydroxide tracer is introduced continuously just below the centrally located, six-bladed turbine impeller, that is into the cylindrical hole (Figure 2) formed by the rotating blades. A variable speed motor drives the impeller; rotational speed is measured by means of a strobotac. The vessel is provided with four, symmetrically placed, 1 in. wide baffles.

Since both acid and base feeds contain a very low concentration of phenolphthalein indicator, a red disk formed by unreacted basic solution engulfs the impeller and extends radially outward (Figure 2). The extent of this zone of reaction is measured visually by means of a wire probe which is positioned by a compound vise assembly. This reaction zone, when viewed vertically (as shown in Figure 2), exhibits the rapidly fluctuating profile of a blow torch flame. An imaginary annulus with inner and outer radii R_1 and R_2 can be drawn coaxial to the impeller shaft so that in the horizontal plane bisecting the impeller blades the red color nearly always fills the disk $r \leq R_1$ but rarely penetrates the zone $r > R_2$. In the present case, for which $R_1 \leq 2.5$ in. and 0.5 in. $< R_2 - R_1 < 0.8$ in., R_1 was chosen to characterize the reaction zone. A small 2-in. impeller was selected to maximize the measurable range of R_1.

Concentration of base and acid feeds and bulk acid in the vessel are obtained by sampling and titration.

Figure 3 presents the variation of reaction zone radius with revolutions per minute at constant acid-base concentration ratio; the data for all runs are included. The obvious expectation that for a given revolution per minute the size of reaction zone should decrease with an increase in acid/base concentration ratio is found in the large majority of cases. A few runs at constant concentration ratio appear to be misplaced; this is probably due to drift in operating conditions during a run. The nearly stoichiometric feeds of acid and base magnifies this effect.

Reaction zone radii are now converted into times for complete reaction by means of Equation (3). Packets of basic tracer are now assumed to be cylinders, and the radii are computed from the above reaction by the use of Toor's equations. Figure 4 indicates the dependence of tracer cylinder radius

Table 1. Radial Velocity Data

Author (Type of impeller)	Impeller radius	Vessel radius	Rev./min.	Separation distance	$\frac{60q_r r}{2\pi r_o^2 q_r}$
Nagata	15 cm.	29 cm.	73	16 cm.	0.81
				18	0.86
(Eight flat-bladed paddle)				20	0.83
				24	0.74
				28	0.43
Manning	2 in.	5 in.	1,500	1.25 in.	1.08
				1.5	0.99
(Six flat-bladed turbine impeller)				1.75	0.97
				2.0	0.93
			900	1.5	1.24
				2.0	1.37
				2.5	1.34
				3.0	1.49
			450	0.75	1.28
				1.0	1.38
				1.25	0.89
				1.5	0.87

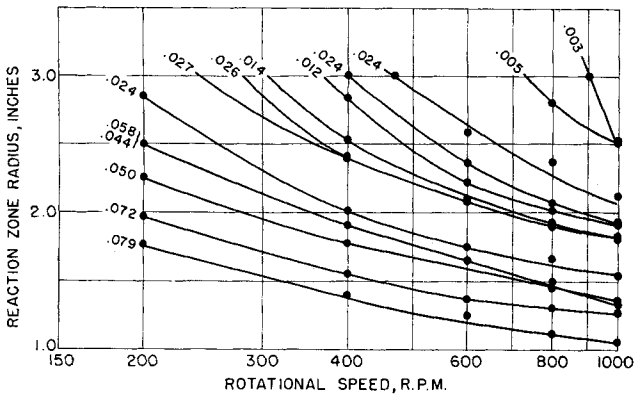

Fig. 3. Reaction zone radius vs. rotational speed.

with rotational speed for a representative sample of the data. The variation of element size with concentration ratio at a constant 800 rev./min. is shown in Figure 5. In all these calculations an average value of the individual acid and base molecular diffusivities was used, for example, 1.5 and 2.0 $\times$ 10^{-5} sq. cm./sec. for the sulfuric acid-sodium hydroxide and nitric acid-sodium hydroxide runs respectively.

DISCUSSION

Reaction times are found to be frequently less than 20 msec.) indicating that the flat-bladed turbine impeller is an extremely efficient mixing device. Under appropriate conditions of acid and base flow rates and concentration the red-colored reaction zone shrinks into the physical confines of the impeller. Here the reaction time is less than the holdup time in the impeller, that is less than 3 msec. at rotational speeds between 600 to 1,000 rev./min.

Figure 4 shows that cylinder radius as calculated from the observed time of reaction is inversely proportional to revolutions per minute. Since the pumping capacity of the impeller is directly proportional to the revolutions per minute, the cylinder radius is seen to be inversely proportional to the volume of recirculating acid with which the fixed volume of tracer is interlarded. However the concentration ratio of acid to base streams affects the results as shown in Figure 5, thus indicating that this simple but crude hypothetical model does not explain exactly the effect of concentration on this complex mixing reaction process. Another method of illustrating this is shown in Figure 6, where computed Z_f are plotted against the concentrations ratio. In this plot Toor's mathematical solutions for slabs, cylinders, and spheres are presented as solid lines, while the present data appear as points and a broken line. However calculation of experimental values of Z_f require

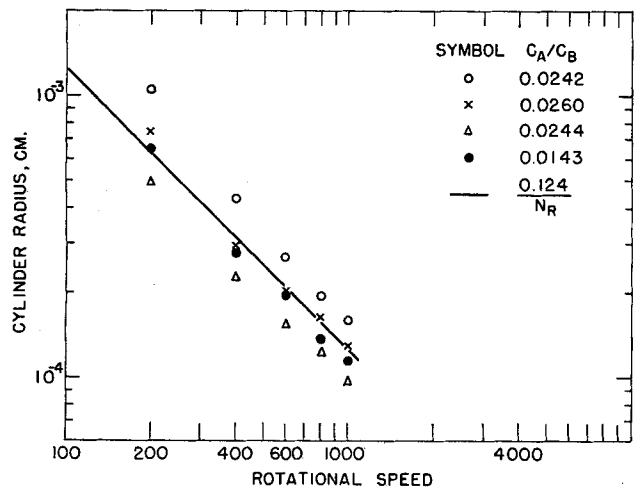

Fig. 4. Cylinder radius vs. rotational speed.

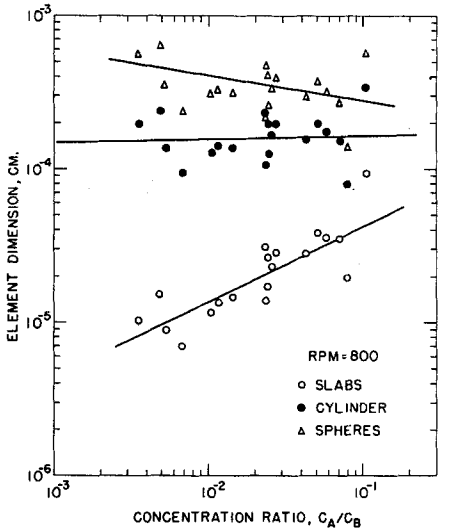

Fig. 5. Element dimension vs. concentration ratio.

an assumption of either a shape (slab, cylinder, or sphere, thus fixing Z_f as a function of C_A/C_B) or the numerical value of the characteristic length of tracer element h. In computing Z_f for use in Figure 6 h was taken equal to $0.124/N_r$ cm. This was done to remove the side effect of revolutions per minute on the desired reaction time—concentration ratio variation. Figure 4 not only justifies this action but also provides the numerical constant. The resulting relative change in experimental Z_f with concentration ratio shows whether the data follow the computed values for slabs, or cylinders, or spheres. Comparison of slopes indicates that the data lie between the sphere and cylinder predictions but are considerably closer to the cylinder.

This crude but simple model for impeller mixing has been tested further as it has been previously applied (*14*) to Manning's data (*7, 8*). This work paralleled the present very closely; instead of reacting a basic tracer with recirculating acid a sodium chloride tracer was mixed with tap water in a similarly shaped stirred vessel (*7*). The resulting concentration fluctuations were measured

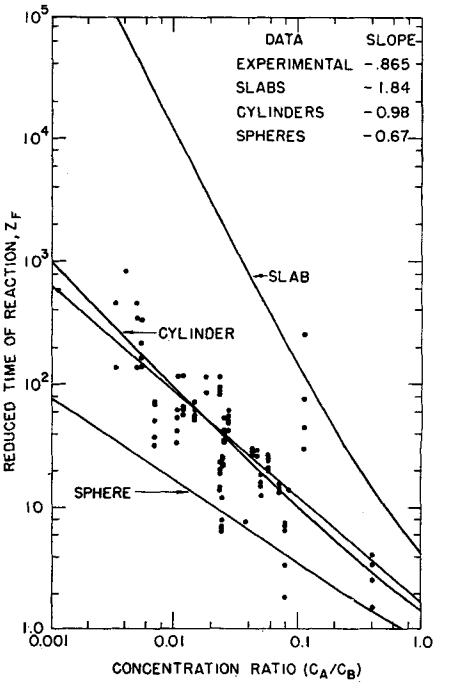

Fig. 6. Comparison of data and theory, time of reaction vs. concentration ratio.

with a specially designed conductivity probe (*6, 7*). Concentration fluctuations were measurable only in the immediate vicinity of the impeller, that is in the region corresponding to the present zone of reaction.

Manning and Wilhelm (*8*) suggested that experimental concentration fluctuations at blade tip positions be obtained by extrapolation, and that these intensities could be compared with an ideal intensity. This ideal intensity is identified as that which would be measured by a probe of very high resolution. It is based on the following model:

1. The recirculation stream entering the impeller from below is substantially at a time average composition C_r determined by the relative flow rates v_t, v_i, and compositions C_t, C_i of the salt tracer stream and of the inlet water stream respectively:

$$C_r = (C_t v_t + C_i v_i)/(v_t + v_i) \qquad (4)$$

2. The time-average composition C_e of the stream leaving the cylinder described by the impeller tips is determined by the relative flow rates v_t, v_r and compositions C_t, C_r of the salt tracer stream and the recirculation stream repectively.

3. Within the confines of the impeller the tracer and recirculating streams become interlarded, and the effluent stream consists of a taffylike composite of the two component streams.

The mean concentration of the exit stream is

$$C_e = (C_r v_r + C_t v_t)/(v_r + v_t) \qquad (5)$$

The ideal root-mean-square fluctuation about this mean concentration is

$$(\Delta C^2_{id})^{1/2} = [\{v_r(C_f - C_e)^2 + v_t(C_t - C_e)^2\}/(v_r + v_t)]^{1/2} \qquad (6)$$

Table 2 provides a comparison between computed ideal intensities and those obtained by extrapolation of intensity data to the blade edges. In this table all quantities were measured directly except recirculation rate and concentrations of tracer in recirculation stream entering and leaving the impeller. Recirculation rate is estimated from the following relationship:

$$\text{Recirculation rate } v_r = \pi^2 d_I^2 N_r d_w \qquad (7)$$

This order of magnitude difference between extrapolated experimental and ideal intensities may be explained by the slab model (*14*). The sodium chloride tracer stream is assumed to be spread out in the form of thin two-dimensional sheets, which are several orders of magnitude thinner than the dimensions of the probe discrimination volume. These thin sheets of tracer stream are intermingled randomly with the bulk recirculation stream. It is impossible for the probe to be surrounded entirely by the tracer stream as the tracer fluid sheets are too thin to fill completely the probe discrimination volume. Therefore the probe cannot see the true tracer concentration volume; as an upper limit it can only see a composite of tracer and surrounding recirculation stream. For the sake of simplicitiy it is assumed that the probe sees only two concentrations, a high value obtained by calculating the

TABLE 2. RANGES OF EXPERIMENTAL VARIABLES

Variable	Range
Impeller size	2 in.
Impeller rotational speed	200 to 1,000 rev./min.
Inlet acid concentration	0.06 to 0.27 *N*
Inlet acid flow rate	7.6 to 15.5 l/min.
Base tracer concentration	0.045 to 0.480 *N*
Base tracer flow rate	0.13 to 0.995 l/min.
Recirculating bulk concentration	0.0008 *N* to 0.0190 *N*
Radius of resulting reaction zone	1 to 3 in.

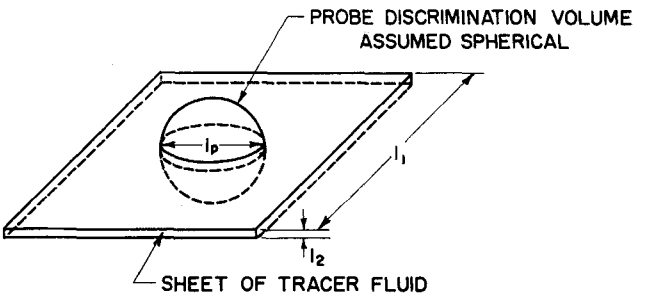

Fig. 7. Illustration of conductivity probe discrimination volume and tracer sheet.

volume-average mean concentration of the fluid in the discrimination volume when it is bisected by one fluid sheet and a low value, the concentration of the recirculation stream. The high concentration C_h is seen from Figure 6 to be

$$C_h = \{C_t(\pi/4)l_p^2 l_2 + C_r(V_p - (\pi/4)l_p^2 l_2)\}/V_p \qquad (8)$$

The probabilities of the probe seeing these two concentration values are assumed to be proportional to the volumes of fluid having these two concentration levels. The high level is seen whenever a tracer slab appears in the probe's discrimination volume, and low reading arises the probe sees only recirculation concentrations. On a unit time basis volume of tracer $v_t = l_2 l_1^2$, where l_1^2 is the area of all tracer slabs produced by the impeller in unit time. The volume of fluid in which the probe will see a tracer slab v_s is the volume swept out by the probe as it follows all the tracer slabs in the effluent stream. From Figure 7

$$v_s = l_1^2 l_p = v_t(l_p/l_2) \qquad (9)$$

Fractional probability P_h of probe seeing high concentration is

$$v_s/(v_r + v_t)$$

Fractional probability P_r of probe seeing low or recirculating stream concentration is $1 - P_h$. The concentration fluctuation intensity ΔC^2_{sm} observed by this probe is

$$\Delta C^2_{sm} = (C_h - C_e)^2 P_h + (C_r - C_e)^2 P_r \qquad (10)$$

where the high concentration is obtained by a material balance

$$C_h = \{v_t C_t + (v_s - v_t)C_r\}/v_s \qquad (11)$$

The concentration fluctuation intensity may now be expressed as a function of the tracer sheet thickness l_2 by combination of Equations (9), (10), and (11). The sheet thickness is now chosen so that the computed concentration fluctuation intensity agrees numerically with the experimentally measured value. Values of tracer sheet thickness for all runs are presented in Table 3. In spite of its crudeness this sheet model leads to two conclusions. First, the probe now sees the high and low concentrations with nearly equal probability, thus producing an approximately symmetrical fluctuation with no extreme fluctuations that extend to the pure tracer concentration value. A probe of very high resolution probably would detect a very symmetrical fluctuation with peaks extending to the tracer concentration value. Second, the sheet thickness decreases as the pumping capacity of the impeller increases, thus agreeing with the obvious expectation that the degree of coarse fluid mixing depends upon the amount of liquid with which the tracer is interlarded and with the previous acid-base reaction results.

Tracer slab thicknesses for the present acid-base reaction results.

Table 3. Comparison of Experimental and Computed Ideal (Maximum) and Tracer Slab Model Concentration Fluctuation Intensities at Impeller Tip

Run no.	1	2	3	4	5	6	7
Impeller diameter, in.	1	1	2	2	2	4	4
Rev./min.	2,860	1,500	1,500	900	450	470	284
Tracer flow rate, v_t, gal./min.	0.05	0.05	0.05	0.05	0.05	0.05	0.05
Water flow rate, v_i, gal./min.	6.5	6.5	6.5	6.5	6.5	6.5	6.5
Recirculation rate, v_r, gal./min.	27	11.4	104	63	31	250	158
Concentration of NaCl in tracer stream, C_t, normality	0.855	0.855	0.855	0.855	0.855	0.855	0.855
Concentration of NaCl in recirculation stream, C_r, normality	0.0065	0.0065	0.0065	0.0065	0.0065	0.0065	0.0065
Mean concentration leaving impeller blade, C_e	0.0081	0.0096	0.0069	0.0072	0.0079	0.0067	0.0068
Ideal computed intensity, %	450	529	267	331	429	179	222
Experimental intensity, %	30	51	20	27	39	11	14
Probe discrimination volume, cu. mm.	0.31	0.31	0.31	0.31	0.31	0.31	0.31
Probability of probe seeing high concentration, %	68	52	45	52	39	49	66
Tracer sheet thickness, cm. $\times 10^{-4}$	3.1	6.0	2.5	3.3	4.5	1.6	2.0

Tracer slab thicknesses for the present acid-base reaction are an order of magnitude smaller than those obtained by extrapolation of concentration fluctuations to the impeller blade tip. In the present work it is assumed that no further stretching of the tracer slabs occur after they leave the impeller; therefore one has calculated an effective or equivalent slab thickness which reacts by diffusion alone in the same time as the actual slabs react by the combined shearing and diffusion processes. This effective thickness should indeed be smaller than the thickness of the elements leaving the impeller.

CONCLUSION

Obviously the present models are extremely crude approaches to the complex problem of fluid dispersion and mixing within a flat-bladed turbine impeller. However the data establish the existence of extremely short times for complete reaction, and these models predict the order of magnitude size of the dispersed and sheared tracer streams. This magnitude is estimated as 10^{-3} to 10^{-5} cm. The acid-base reaction data favor cylindrical or spherical shapes, while the tracer studies predict slab shapes.

NOTATION

C_A = concentration of acid in tank, normality
C_B = concentration of base in tracer, normality
C_e = concentration of sodium chloride tracer in stream leaving impeller
C_h = high concentration value seen by conductivity probe
C_l = low concentration value seen by conductivity probe
C_r = concentration of sodium chloride tracer in recirculating stream
C_t = concentration of sodium chloride in tracer stream
ΔC_{sm} = calculated concentration fluctuation intensity with tracer sheet model
D = molecular diffusivity
d_I = diameter of flat-bladed turbine impeller
d_W = blade width of flat-bladed turbine impeller
h = characteristic length of tracer element, that is slab half thickness, cylinder radius, or sphere radius, cm.
K = proportionality constant in Equation (1)
l_p = characteristic dimension of conductivity probe discrimination volume
l_1^2 = average area of tracer fluid sheet, on a unit time basis
l_2 = average thickness of tracer fluid sheet
N_r = impeller rotational speed, rev./min.
P_h = probability that conductivity probe sees a tracer slab
P_r = probability that conductivity probe sees only recirculating fluid
R_1 = inner radius of imaginary annulus that surrounds red-colored reaction zone, in.
R_2 = outer radius of imaginary annulus that surrounds red-colored reaction zone, in.
r = radial distance from center of impeller
r_o = radius of flat-bladed turbine impeller
q = radial velocity of fluid
t = time for complete reaction, sec.
V_p = $(\pi/6)_p^3$, conductivity probe discrimination volume
v_i = volume of tap water fed into vessel per unit time
v_r = estimated pumping capacity of impeller
v_s = volume swept out by conductivity probe on a unit time basis
v_t = volume of sodium chloride tracer fed into vessel per unit time
X = radial distance from center of mixing vessel
Y = element of vertical distance
Z_f = $4\ D\ t/h^2$, reduced time of reaction dimensionless group
β = C_A/C_B, concentration ratio dimensionless group

LITERATURE CITED

1. Batchelor, G. K., *J. Fluid Mech.*, **5**, 113 (1959).
2. ———, I. D. Howells, and A. A. Townsend, *ibid.*, p. 134.
3. Beek, J., Jr., and R. S. Miller, *Chem. Eng. Progr. Symposium Ser. No. 25*, **55**, 23 (1959).
4. Corrsin, S., *A.I.Ch.E. Journal*, **3**, 329 (1957).
5. Kramers, H., G. M. Baars, and W. H. Knoll, *Chem. Eng. Sci.*, **2**, 35 (1953).
6. Lamb, D. E., F. S. Manning, and R. H. Wilhelm, *A.I.Ch.E. Journal*, **6**, 682 (1960).
7. Manning, F. S., Ph.D. dissertation, Princeton Univ., Princeton, New Jersey (1959).
8. ———, and R. H. Wilhelm, *A.I.Ch.E. Journal*, **9**, 12 (1963).
9. Nagata, *Mem. Fac. Eng. Kyoto Univ.*, **21**, No. 3, p. 265 (1959).
10. Rice, A. W., M.S. thesis, Carnegie Institute of Technology, Pittsburgh, Pennsylvania (1962).
11. Rushton, J. H., E. W. Costich, and H. J. Everett, *Chem. Eng. Progr.*, **46**, 395, 467 (1950).
12. Toor, H. L., *A.I.Ch.E. Journal*, **8**, 70 (1962).
13. van de Vusse, J. G., *Chem. Eng. Sci.*, **4**, 178 (1955).
14. Wilhelm, R. H., Private communication.

Manuscript received November 7, 1962; revision received July 22, 1963; paper accepted July 23, 1963. Paper presented at A.I.Ch.E. Chicago meeting.